Irregular stacking sequence in the initial growth of ultrathin Rh films on Ru(0001)

Yunbin He,[1,*] Ari P. Seitsonen,[2] and Herbert Over[1,†]
[1]*Physikalisch Chemisches Institut, Justus-Liebig-Universität Giessen, Heinrich-Buff-Ring 58, 35392 Giessen, Germany*
[2]*Physikalisch Chemisches Institut, Universität Zürich, Winterthurerstrasse. 190, CH-8057 Zürich, Switzerland*
(Received 20 March 2005; published 19 August 2005)

Rhodium grows on single-crystal Ru(0001) surface initially layer by layer, adapting the in-plane lattice parameters of Ru(0001) (pseudomorphic growth). Using quantitative low-energy electron diffraction (LEED) and density functional theory (DFT) calculations, we determined the atomic structures of 1-monolayer (ML), 2-ML, and 3-ML Rh films on Ru(0001). The 1-ML Rh film continues the hexagonal-close-packed (hcp) stacking sequence of Ru(0001) (…*ABAb*), while the 2-ML Rh film already adopts its face-centered-cubic (fcc) stacking sequence (…*ABAbc*) if the topmost Ru layer is included into the stacking consideration. Three MLs of Rh form a fcc stacking sequence of …*ABAbac*, requiring a massive restructuring of the second Rh layer when adding one ML of Rh onto the 2-ML Rh film.

DOI: 10.1103/PhysRevB.72.075432 PACS number(s): 68.35.Ct, 68.35.Rh, 61.14.Hg

I. INTRODUCTION

Ultrathin metal films of only a few monolayers thickness grown on a dissimilar metal surface may dramatically change the physical and chemical surface properties, such as the surface catalytic activity or the magnetization.[1] This prospect triggers technological efforts in the fabrication of ultrathin metal-on-metal films. From a scientific point of view, such metal-on-metal films are ideal systems for a detailed investigation of the initial growth mode and the interfacial structure, both of which are key issues in epitaxy.[2]

There are three well-established growth modes for epitaxy: (i) Frank–van der Merwe (FM) or the two-dimensional (also called layer-by-layer) mode, (ii) Volmer-Weber (VW) or the three-dimensional mode, and (iii) Stranski-Krastanov (SK) or the two-dimensional mode followed by the three-dimensional mode.[3] According to the quasiequilibrium description by Bauer,[4] these three growth modes are governed by surface free energies of the film and substrate, the interface free energy, and the strain energy. If the deposited ultrathin metal film adapts the planar lattice constants of the substrate surface, the epitaxial growth is referred to as pseudomorphic epitaxy. As yet, pseudomorphic epitaxial growth has been observed in various bimetallic systems, to name only a few, fcc/fcc: Ag/Pd(111),[5] Pt/Ni(111),[6] Rh/Ag{001},[7] Cu/Pt{001},[8] Ni/Cu(001);[9] bcc/fcc: Fe on Au{001},[10] Rh{001},[11] Pd{001},[12] Cu{111},[13] and Ni(111),[14] Mn/Pd(111),[15] V/Cu(001);[16] bcc/bcc: Mn on V(001)[17] and Fe(001);[18] fcc/hcp: Cu,[19] Ni,[20] Au and Pd[21] on Ru(0001), Cu/Co(0001),[22] Ag/Re(0001);[23] hcp/bcc: Co/Fe(001);[24] hcp/hcp: Cd/Ti(0001);[25] hcp/fcc: Co/Cu(111).[26,27]

In this paper we focus on the initial growth and structural properties of a particularly interesting system, namely ultrathin Rh films on Ru(0001). While rhodium crystallizes in the fcc structure with a stacking sequence *abcabc*…, ruthenium stacks in the hcp sequence of *ABAB*…. The small in-plane lattice misfit of 0.7% between fcc Rh(111) (a_{Rh}=2.69 Å) and hcp Ru(0001) (a_{Ru}=2.71 Å) forces the epitaxial growth to proceed in a pseudomorphic way, i.e., the in-plane lattice constants of the Rh film are identical to those of the Ru(0001) substrate. For an analogous bimetallic fcc/hcp system, Cu/Ru(0001),[19] it was reported that, despite a relatively large (5.8%) in-plain lattice misfit between the film and substrate, one-monolayer (1 ML) Cu grows pseudomorphically and continues the hcp stacking of the Ru(0001) substrate. At a thickness of 2 MLs, the Cu film is reconstructed to form a uniaxially compressed stripe phase, consisting of regions of faulted fcc and hcp stacking separated by stripes of dislocations. On the bimetallic system, Co/Cu(111) (hcp/fcc),[26,27] it was reported that, the first two MLs of Co grow pseudomorphically in a layer-by-layer mode, continuing the fcc stacking of the Cu(111) substrate, and for the subsequent layers the hcp structure starts to grow with possible admixture of fcc stacking. Pure hcp stacking develops for layers thicker than around five MLs. However, the hcp stacking switches back to fcc when the cobalt film is sandwiched by further deposition of copper. At least the top cobalt layer undergoes a full registry shift from hcp to fcc sites. Similar thickness-dependent structural transformation has been observed in Ru-Ir (hcp-fcc) superlattice, where it was found that Ir is in hcp when thicker Ru layers dominate the mean structure of the coherent epitaxial assembly and fcc when Ir are dominant. Such thickness-induced hcp-fcc transition in metals and metallic superlattices has been theoretically discussed by Zangwill and co-workers.[28]

Turning back to our specific bimetallic system of Rh/Ru(0001), several questions arise: When and how will the Rh film establish its own fcc stacking sequence on the hcp Ru(0001) surface with progressing thickness and what are the structural parameters? How does the intermixing between Rh and Ru influence the stacking sequence of the resulting composite Rh-Ru film? In the present work, based on both quantitative low-energy electron diffraction (LEED) and density functional theory (DFT) calculations, we have firmly resolved these questions, and found a thickness-induced change of the stacking sequence, i.e., a registry shift of the second Rh layer when the film thickness varies from 2 ML to 3 ML of Rh.

II. EXPERIMENT AND DFT CALCULATION

Evaporation of Rh layers on single-crystal Ru(0001) was carried out with a well-outgassed electron-beam evaporator in an ultrahigh vacuum (UHV) chamber; during Rh evaporation the base pressure was 2×10^{-10} mbar. The chamber is additionally equipped with four-grid LEED optics, a quadrupole mass spectrometer for thermal desorption spectroscopy (TDS), and facilities for Auger electron spectroscopy (AES) and surface cleaning. Prior to the Rh film deposition, the Ru(0001) substrate was cleaned by cycles of argon ion sputtering and flashing up to 1400 K. Rhodium was evaporated from a well-outgassed source consisting of a short Rh rod (diameter: 1 mm, purity: 99.5% supplied by ChemPure) by electron-beam bombardment. The evaporation rate of Rh can be controlled by the Rh ion flux during evaporation. Since the evaporation cell is contained in a water-cooled shroud, the heating is essentially confined to the Rh rod, which keeps the background pressure in the chamber during evaporation still in the low 10^{-10} mbar pressure regime. During Rh evaporation a substrate temperature of 650 K was chosen to avoid contamination of the substrate surface from residual gases such as CO, H_2, and H_2O, and to facilitate a layer-by-layer growth of Rh on Ru(0001) without inducing a significant intermixing and/or alloying between Ru and Rh. At a sample temperature of 650 K, the deposited Rh film on the Ru(0001) substrate surface is considered to be in thermodynamic equilibrium. Substantial intermixing of Rh and Ru occurs only above 750 K.

For the DFT calculations,[29] we employed the generalized gradient approximation (GGA) of Perdew, Burke, and Ernzerhof[30] for the exchange-correlation functional. The electronic wave functions were expanded in a plane-wave basis set with an energy cutoff of 21 Ry. The surface was modeled by nine independent layers of Ru(0001) and setting various pseudomorphic Rh layers on both sides of the slab (supercell approach). The in-plane lattice parameter was 2.726 Å. The length of the unit cell parallel to the surface normal was kept fixed, making sure that consecutive Rh-Ru(0001) slabs were separated by a vacuum region of at least 9.6 Å. We relaxed the atomic coordinates of the top two layers on each side of the slab. A 12×12 Monkhorst-Pack k point mesh centered at Γ point was used to approximate the integrals over the reciprocal space, giving 19 points in the irreducible wedge of the Brillouin zone. We checked these numerical parameters to be sufficient to extract reliable energies and geometries.

III. RESULTS AND DISCUSSION

After Rh deposition, AES was employed to monitor the surface cleanliness of the Rh films, to calibrate the deposition rate, as well as to determine the growth mechanism. All AES measurements were performed at room temperature. Auger lines of Ru (273 eV) and Rh (302 eV) were taken for quantitative analysis. In Fig. 1 the normalized AES peak-to-peak height of Rh (302 eV) versus the deposition time is presented. The so-called "Auger breaks" are clearly visible in the plot at 6 and 12 min, which suggests a layer-by-layer growth mode of Rh on Ru(0001). Layer-by-layer growth mode of Rh on Ru(0001) is already expected from the small in-plane lattice mismatch of both materials (2.69 Å versus 2.71 Å). The Auger breaks allow also a precise determination of the 1-ML Rh coverage and thus for a calibration of the deposition rate for a constant Rh ion flux of 32 nA. The first monolayer of Rh was completed after 6 min of evaporation, the second layer after 12 min, consistent with the deposition time of the first Rh layer.

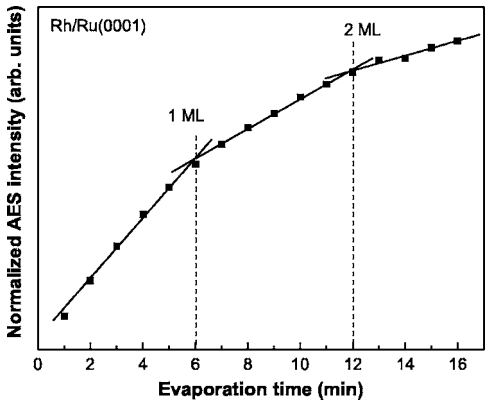

FIG. 1. The AES peak-to-peak heights of Rh (302 eV) normalized to the sum of peak-to-peak heights of Ru (273 eV) and Rh (302 eV), taking sensitivity factors into account, are shown as a function of the Rh deposition time. The dashed lines at evaporation times of 6 min and 12 min, marking the Auger breaks, correspond to 1 ML and 2 ML of Rh growth, respectively.

The layer-by-layer growth mode and the calibration of 1-ML Rh coverage were further corroborated by LEED experiments. We deposited the Rh layers in equidistant time step of 60 sec (sample temperature 650 K) and recorded the respective LEED patterns at a fixed electron beam energy of 89 eV and at room temperature until about 2 MLs of Rh were grown on Ru(0001). The integral LEED intensities of the (10) beam were normalized to the background intensity and are displayed in Fig. 2 as a function of the deposition time. This LEED intensity ratio depends critically on the roughness of the Rh film analogous to reflection high-energy electron diffraction (RHEED) oscillations typically observed during layer-by-layer growth.[31] The observed oscillatory behavior of the LEED intensity as a function of the deposition time in Fig. 2 confirms a layer-by-layer growth mode of Rh on Ru(0001).[32] The first Rh monolayer was completed after 6 min of Rh deposition, which is in nice agreement with the AES results, thus providing additional confidence to the 1-ML Rh calibration.

The Rh-Ru(0001) system shows always a sixfold symmetric pattern in LEED. If the pure Ru(0001) surface consists of a single terrace, then the LEED pattern would be only of threefold symmetry. However, the clean Ru(0001) surface has many single atomic steps and the surface unit cells of adjacent terraces are rotated by 60°. Therefore LEED reveals always a sixfold symmetric pattern.[27] Quite in contrast, fcc(111) surfaces normally lead to threefold symmetric LEED patterns. The dimensions of the unit cells of adjacent terraces, which are separated by a single step, are identical. Therefore, as soon as the Rh film establishes a single abc

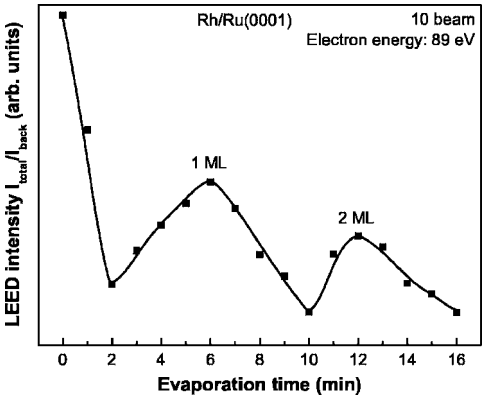

FIG. 2. RHEED-like oscillations of the LEED intensity of the (10) beam normalized to the background intensity as a function of the Rh deposition time. At 6 min and 12 min the normalized LEED intensity exhibits maxima, i.e., the roughness of the Rh-Ru(0001) surface is minimal, indicative of 1 ML and 2 ML of Rh, respectively. The solid line is a guide to the eye.

stacking sequence, we should observe a threefold symmetric pattern on the LEED screen. Altogether the appearance of a sixfold symmetric LEED pattern for the Rh-Ru(0001) system indicates either the presence of fcc stacking of Rh twins, which are rotated by 60° or the presence of hcp stacking of Rh on the Ru(0001) surface.

With the calibration of one ML of Rh, we are able to produce reliably and reproducibly Rh films with predefined thickness. In what follows we discuss the atomic geometries of 1-ML, 2-ML, and 3-ML Rh films on Ru(0001) using quantitative LEED. We measured for each Rh film a full LEED intensity data set, comprising three beams in the energy range of 80 eV to 430 eV. The accumulative energy range was 790 eV. The atomic phase shifts of Ru and Rh are practically identical. Still we should be able to discriminate between a Rh layer and a Ru layer due to the different layer spacings. In bulk Rh(111) the layer spacing is 2.19 Å, while in Ru(0001) the interlayer distance is 2.14 Å. LEED intensity simulations were performed with the LEED program package developed by W. Moritz and co-workers.[33] The comparison between the experimental and calculated LEED *I-V* curves was quantified by using Pendry's *r* factor.[34] The experimental LEED data were fitted in an automatic way, applying a least-squares optimization scheme. The main structural parameters derived by the LEED analyses are the stacking sequence of the Rh layers with respect to the Ru(0001) substrate and the corresponding layer spacings. The structural results are summarized in Fig. 3. The agreement between experimental and calculated LEED intensity data can be judged from Fig. 4. In all cases the optimum *r*-factor values were between 0.16 and 0.18, which signifies a good agreement between experimental and calculated LEED *I-V* data (cf. Fig. 4).

In the 1-ML Rh film the Rh-Ru layer distance is 2.17 Å, which is close to that of bulk Rh(111), while the topmost Ru layer spacing is still slightly contracted as for the clean Ru(0001) surface. The topmost Ru-Ru layer distance is 2.11 Å, a layer distance that has been found for all grown Rh films. Obviously the capping Rh layer does not affect the

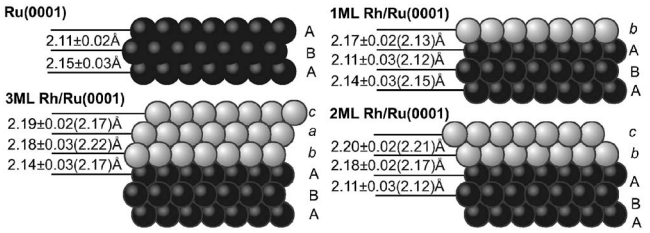

FIG. 3. Structural results of the clean and Rh-covered Ru(0001) surfaces. Rh grows pseudomorphically on Ru(0001). The structural parameters are determined by quantitative LEED and by DFT calculations (values in parentheses).

layer distances in the Ru(0001) substrate, a quite remarkable result as one would expect that the capping Rh layer transforms the topmost Ru layer into a bulklike Ru layer with a Ru-Ru layer distance close to the bulk value of 2.14 Å. The topmost Rh-Rh layer distance in the 2-ML Rh film is 2.20 Å and is therefore slightly expanded with respect to Rh(111), the next Rh-Ru layer distance is similar to the value found for the 1-ML Rh film. The stacking sequence (…*ABA**bc***) is already fcc-like when the topmost Ru layer is included into the stacking consideration. The 3-ML Rh film has already built up its own Rh fcc stacking sequence (…*ABA**bac***). The interlayer distances between the three Rh layers are again almost Rh(111) bulklike.

The most surprising result of the structural LEED analyses is the change in the stacking sequence of the Rh layers when turning from the 2-ML Rh film to the 3-ML Rh film. For all cases studied the first Rh layer on Ru(0001) continues the imposed Ru hcp stacking (…*ABAb*). However, the registry of the second Rh layer depends on the film thickness. For the 2-ML Rh film, the second Rh layer is in the fcc position (…*ABA**bc***). The sixfold symmetry of the LEED pattern indicates the formation of twins, each rotated by 60°. In contrast, the second Rh layer in the 3-ML Rh film switches back to the hcp stacking of Ru(0001) (…*ABA**ba***). This registry shift of the second Rh layer is quite unexpected and

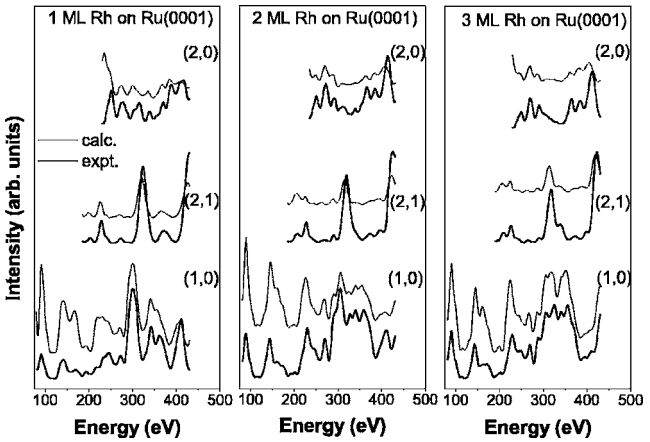

FIG. 4. Comparison of calculated and experimental LEED *I-V* data for 1-ML, 2-ML, and 3-ML Rh films on Ru(0001). The overall agreement is quantified by Pendry's reliability factors of 0.16–0.18, a value which is considered to be a good experiment and/or theory agreement.

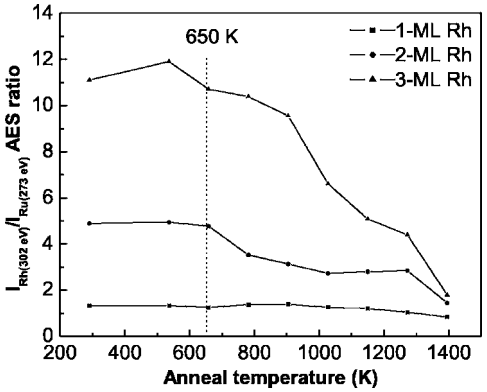

FIG. 5. AES ratio of Rh(302 eV)/Ru(273 eV) as a function of the anneal temperature for the 1-ML, 2-ML, and 3-ML Rh films which were prepared at room temperature. The vertical dash line corresponds to 650 K, at which temperature, ultrathin Rh films are normally evaporated on the Ru(0001) substrate.

different from the hcp-fcc transitions occurring in the Co/Cu(111) system. In the Co/Cu(111) system the stacking fault in the Co film is induced by a Cu cap layer.[26,27] For the Rh/Ru(0001) system the Rh film is not capped by a Ru layer as long as the preparation temperature is 650 K or below. In Fig. 5, the AES ratio of Rh(302 eV)/Ru(273 eV) is shown as a function of the anneal temperature for the 1-ML, 2-ML, and 3-ML Rh films which were initially deposited at room temperature (RT). It is obvious that in all cases the AES ratio remains almost constant when the film is annealed from RT to 650 K, indicating there is no significant intermixing of Ru and Rh, and no Ru layer capping on the Rh layers. DFT calculations substantiate as well this view. If a Ru layer is capping the Rh film, then the topmost layer distance turned out to be 2.11 Å, while a Rh film without a Ru capping layer reveals a layer distance of 2.20 Å. This latter value is also found with quantitative LEED (2.20 Å), thus excluding the presence of a Ru cap layer. But also the total energies exclude the presence of a Ru capping layer. The energy per (1×1) unit cell increases by 400 meV when a Ru layer is capping the Rh film.

The third Rh layer in the 3-ML Rh film completes the fcc stacking of Rh (…*ABA**bac***). The 4-ML Rh film reveals a stacking sequence (…*ABAbacb*), which is expected when starting from the 3-ML Rh film geometry. Since the sample temperature during Rh evaporation was 650 K, we assume that all Rh films constitute equilibrium configurations.

Why are the geometries of the 2-ML Rh film and the 3-ML Rh film so surprising? Assuming that one has prepared a 2-ML Rh film on Ru(0001) at 650 K (…*ABA**bc***) first, subsequently reduces the sample temperature to room temperature or lower and then evaporates an additional Rh layer on top of the 2-ML Rh film. The result should be that the topmost Rh layer will follow the sequence (…*ABA**bca***), which is different from the equilibrium sequence (…*ABA**bac***). Indeed the metastable Rh film (…*ABA**bca***) has been identified with quantitative LEED, corroborating the specific role of the 2-ML Rh film.

With DFT calculations, we studied the energetics of the pseudomorphic Rh film growth on Ru(0001). Table I summarizes the energy differences for the Rh films of various thicknesses and stacking sequences; the hcp stacking sequence serves as the reference point. For the 1-ML Rh film, Rh continues the hcp stacking (…*ABAb*) which is by 139 meV per surface unit cell more favorable than the fcc stacking sequence (…*ABAc*). The energy difference between the competing stacking sequences (…*ABAba*) and (…*ABAbc*) for the 2-ML Rh film is practically degenerate (energy difference is as low as 0.6 meV in favor of …*ABAbc*). Fortunately, the quantitative LEED analysis result identifies firmly the (…*ABAbc*) stacking sequence. For the 3-ML Rh film, the energy difference between the hcp (…*ABAbab*) and fcc (…*ABAbac*) stacking is 53 meV in favor of the fcc stacking. In addition the fcc (…*ABA**bac***) is by 70 meV more favorable than the fcc (…*ABA**bca***) stacking sequence. Both energy differences are surprisingly high. Altogether, DFT calculations confirm clearly the stacking sequence (…*ABA**bac***) for the 3-ML Rh film on Ru(0001) as identified by LEED analyses. We speculate that the energy degeneracy of the (…*ABAbc*) and (…*ABAba*) facilitates the stacking (…*ABAbac*) of the 3-ML Rh growth. The structural parameters for the 1-ML, 2-ML, and 3-ML Rh films are in-

TABLE I. DFT derived energy differences and LEED *I-V* analysis derived Pendry's *r* factors (R_p) for the Rh films on Ru(0001) of various thicknesses and stacking sequences. The hcp stacking sequence serves as the reference point for the DFT energy calculation. Bold values indicate those which are favored in terms of total energy (DFT) or Pendry's *r*-factor values (LEED).

	DFT Energy Difference (meV/unit cell)		R_p of LEED-$I(V)$	
Rh on Ru(0001)	hcp	fcc	hcp	fcc
1 ML	…*ABAb*	…*ABAc*	…*ABAb*	…*ABAc*
	0	+139.2	**0.18**	0.68
2 ML	…*ABAba*	…*ABAbc*	…*ABAba*	…*ABAbc*
	0	**−0.6**	0.51	**0.18**
3 ML	…*ABAbab*	…*ABAbac*	…*ABAbab*	…*ABAbac*
	0	**−53**	0.48	**0.16**
		…*ABAbca*		…*ABAbca*
		+17		0.45

dicated in Fig. 3 in parentheses. These values agree well with the LEED derived values.

In a last experiment we studied the intermixing of Rh and Ru in the near-surface region for the 3-ML Rh film on Ru(0001). Substantial intermixing of Ru and Rh sets in at about 750 K (cf. Fig. 5). Still the once established stacking sequence (…*ABAbac*) is preserved. However, if the annealing temperature is raised to 1400 K, not only substantial intermixing of Rh and Ru is observed in AES, but also the stacking sequence changes from fcc to hcp, as revealed by a quantitative LEED analysis. The concentration of Ru in the surface region is estimated to be around 50%. This result is consistent with recent DFT calculations where the fcc Rh phase is stable up to 40% of Ru and beyond this concentration hcp is more stable.[35] The topmost layer spacing of the heavily annealed Rh film is around 2.19 Å. The AES ratio of Rh(302 eV)/Ru(273 eV) remains about 2, excluding a pure Ru cap layer on the heavily intermixed film. The driving force for the fcc-hcp stacking switch in the heavily intermixed Rh-Ru(0001) system is yet unclear, but appears to be different from that for the Co/Cu(111) system in which the Cu capping layer induces the hcp-fcc stacking switch of the Co layers.[26,27]

IV. SUMMARY AND CONCLUSION

In summary, at a sample temperature of 650 K, rhodium grows initially layer-by-layer and pseudomorphically on a single-crystal Ru(0001) substrate. It is revealed by quantitative LEED that a 1-ML Rh film continues the hcp stacking of Rh(0001) (…*ABA**b***), while the 2-ML Rh film already establishes fcc stacking (…*ABA**bc***) if including the topmost Ru layer into the stacking consideration. Very interestingly, in the 3-ML Rh film, the third Rh layer induces a rearrangement of the second Rh layer such that it stacks in …*ABA**bac*** instead of …*ABAbca*, which is initially expected from the atomic geometry of the 2-ML Rh film. DFT calculations corroborate the findings from quantitative LEED analyses.

ACKNOWLEDGMENTS

We acknowledge partial financial support from the European Union under Contract No. NMP3-CT-2003-505670 (NANO2). We are grateful to the Leibniz-Rechenzentrum in Munich for providing us with computing time. We thank S. Curtarolo for providing us with Ref. 35(a) prior to publication and Franco Jona for fruitful discussions.

*Corresponding author. FAX: ++49-641-9934559. Email address: Yunbin.He@phys.chemie.uni-giessen.de

†Corresponding author. FAX: ++49-641-9934559. Email address: Herbert.Over@phys.Chemie.uni-giessen.de; URL: http://www.chemie.uni-giessen.de/home/over

[1] J. A. Rodriguez and D. W. Goodman, Science **257**, 897 (1992); J. A. Rodriguez, Surf. Sci. Rep. **24**, 223 (1996); G. Ertl, H. Knözinger, and J. Weitkamp, *Handbook of Heterogeneous Catalysis* (VCH, Weinheim, 1997).

[2] H. Brune, Surf. Sci. Rep. **31**, 121 (1998).

[3] A. Zangwill, *Physics at Surfaces* (Cambridge University Press, Cambridge, UK, 1988).

[4] E. Bauer, Appl. Surf. Sci. **11/12**, 479 (1982).

[5] B. Eisenhut, J. Stober, G. Rangelov, and T. Fauster, Phys. Rev. B **47**, 12980 (1993).

[6] O. Robach, H. Isern, P. Steadman, K. F. Peters, C. Quiros, and S. Ferrer, Phys. Rev. B **68**, 214416 (2003).

[7] H. Li, S. C. Wu, D. Tian, Y. S. Li, J. Quinn, and F. Jona, Phys. Rev. B **44**, 1438 (1991).

[8] Y. S. Li, J. Quinn, H. Li, D. Tian, F. Jona, and P. M. Marcus, Phys. Rev. B **44**, 8261 (1991).

[9] W. Platow, U. Bovensiepen, P. Poulopoulos, M. Farle, K. Baberschke, L. Hammer, S. Walter, S. Müller, and K. Heinz, Phys. Rev. B **59**, 12641 (1999).

[10] A. M. Begley, S. K. Kim, J. Quinn, F. Jona, H. Over, and P. M. Marcus, Phys. Rev. B **48**, 1779 (1993).

[11] A. M. Begley, S. K. Kim, F. Jona, and P. M. Marcus, Phys. Rev. B **48**, 1786 (1993).

[12] J. Quinn, Y. S. Li, H. Li, D. Tian, F. Jona, and P. M. Marcus, Phys. Rev. B **43**, 3959 (1991).

[13] D. Tian, F. Jona, and P. M. Marcus, Phys. Rev. B **45**, 11216 (1992).

[14] G. C. Gazzadi, F. Bruno, R. Capelli, L. Pasquali, and S. Nannarone, Phys. Rev. B **65**, 205417 (2002).

[15] D. Tian, H. Li, S. C. Wu, F. Jona, and P. M. Marcus, Phys. Rev. B **45**, 3749 (1992).

[16] Y. Tian, F. Jona, and P. M. Marcus, Phys. Rev. B **59**, 12286 (1999).

[17] Y. Tian, F. Jona, and P. M. Marcus, Phys. Rev. B **59**, 12647 (1999).

[18] S. K. Kim, Y. Tian, M. Montesano, F. Jona, and P. M. Marcus, Phys. Rev. B **54**, 5081 (1996).

[19] C. Günther, J. Vrijmoeth, R. Q. Hwang, and R. J. Behm, Phys. Rev. Lett. **74**, 754 (1995); H. Zajonz, A. P. Baddorf, Doon Gibbs, and D. M. Zehner, Phys. Rev. B **62**, 10436 (2000); G. O. Pötschke and R. J. Behm, *ibid.* **44**, 1442 (1991); H. Zajonz, D. Gibbs, A. P. Baddorf, V. Jahns, and D. M. Zehner, Surf. Sci. **447**, L141 (2000); Ch. Ammer, K. Meinel, H. Wolter, A. Beckmann, and H. Neddermeyer, *ibid.* **375**, 302 (1997); S. D. Ruebush, R. E. Couch, S. Thevuthasan, and C. S. Fadley, *ibid.* **421**, 205 (1999).

[20] D. G. O'Neill and J. E. Houston, Phys. Rev. B **42**, 2792 (1990).

[21] A. Steltenpohl, N. Memmel, E. Taglauer, Th. Fauster, and J. Onsgaard, Surf. Sci. **382**, 300 (1997).

[22] J. E. Prieto, Ch. Rath, S. Müller, R. Miranda, and K. Heinz, Surf. Sci. **401**, 248 (1998).

[23] M. Parschau, D. Schlatterbeck, and K. Christmann, Surf. Sci. **376**, 133 (1997).

[24] S. K. Kim, C. Petersen, F. Jona, and P. M. Marcus, Phys. Rev. B **54**, 2184 (1996).

[25] H. D. Shih, F. Jona, D. W. Jepsen, and P. M. Marcus, Phys. Rev. B **15**, 5550 (1977); H. D. Shih, F. Jona, D. W. Jepsen, and P. M. Marcus, *ibid.* **15**, 5561 (1977).

[26] Ch. Rath, J. E. Prieto, S. Müller, R. Miranda, and K. Heinz, Phys.

Rev. B **55**, 10791 (1997); M. Hochstrasser, M. Zurkirch, M. Erbudak, E. Wetli, and D. Pescia, J. Magn. Magn. Mater. **148**, 4 (1995); Y. Wang, X. W. Li, J. F. Jia, H. Ji, Y. Yang, H. Gul Bahar, S. C. Wu, and R. G. Zhao, Surf. Sci. **375**, 226 (1997); S. Müller, G. Kostka, T. Schäfer, J. de la Figuera, J. E. Prieto, C. Ocal, R. Miranda, K. Heinz, and K. Müller, *ibid.* **352-354**, 46 (1996); J. de la Figuera, J. E. Prieto, G. Kostka, S. Müller, C. Ocal, R. Miranda, and K. Heinz, *ibid.* **349**, L139 (1996).

[27] B. P. Tonner, Z.-L. Han, and J. Zhang, Phys. Rev. B **47**, 9723 (1993).

[28] A. C. Redfield and A. M. Zangwill, Phys. Rev. B **34**, 1378 (1986); R. Bruinsma and A. Zangwill, Phys. Rev. Lett. **55**, 214 (1985).

[29] The calculations were performed with the program VASP [G. Kresse and J. Furthmüller, Comput. Mater. Sci. **6**, 15 (1996); Phys. Rev. B **54**, 11169 (1996)] and employing the projected augmented wave (PAW)[P. E. Blöchl, *ibid.* **50**, 17953 (1994)] approach in the variant of Kresse and Joubert; [G. Kresse and J. Joubert, Phys. Rev. B **59**, 1758 (1999)] to describe the action of the core electrons on the valence electrons and to remove the divergence in the external potential. The PAWs were taken from the standard library coming with the code.

[30] J. P. Perdew, K. Burke, and M. Ernzerhof, Phys. Rev. Lett. **77**, 3865 (1996).

[31] W. F. Egelhoff, Jr., and I. Jacob, Phys. Rev. Lett. **62**, 921 (1989).

[32] D. K. Flynn, W. Wang, S. L. Chang, M. C. Tringides, and P. A. Thiel, Langmuir **4**, 1096 (1988).

[33] W. Moritz, J. Phys. C **17**, 353 (1984); G. Kleinle, W. Moritz, and G. Ertl, Surf. Sci. **226**, 119 (1990); H. Over, U. Ketterl, W. Moritz, and G. Ertl, Phys. Rev. B **46**, 15438 (1992).

[34] J. B. Pendry, J. Phys. C **13**, 937 (1980).

[35] S. Curtarolo, D. Morgan, and G. Ceder, Meas. Sci. Technol. **16**, 296–301 (2005). All calculations are also available online: http://datamine.mit.edu; S. Curtarolo, D. Morgan, K. Persson, J. Rodgers, and G. Ceder, Phys. Rev. Lett. **91**, 135503 (2003).